

DISCRETE SURFACE LIGHT BULLETS

D. MIHALACHE, D. MAZILU

*“Horia Hulubei” National Institute for Physics and Nuclear Engineering (IFIN-HH),
Department of Theoretical Physics,
407 Atomistilor, Magurele-Bucharest, 077125, Romania
E-mail: Dumitru.Mihalache@nipne.ro*

(Received January 8, 2009)

Abstract. We give an overview of recent results obtained in the study of discrete surface spatiotemporal optical solitons (“discrete surface light bullets”). We analyze spatiotemporal light localization near the edges of semi-infinite arrays of weakly coupled nonlinear waveguides and in the corners or at the edges of truncated two-dimensional photonic lattices and demonstrate the existence of novel classes of continuous-discrete spatiotemporal optical solitons. We study the existence and stability of the families of discrete surface light bullets and compare their properties with those of the spatiotemporal nonlinear modes located deep inside the one- and two-dimensional photonic lattices.

Key words: spatiotemporal optical solitons, light bullets, discrete solitons, surface solitons.

1. INTRODUCTION

In the past years there has been an increasing interest in the study of localized structures of light, which defy either diffraction or dispersion and represent the particle-like counterpart of the more common nonlocalized (extended) light structures. *Optical solitons* are packets of localized electromagnetic radiation that propagate without spreading out despite diffraction or group-velocity dispersion (GVD) [1–5]. The optical media that might sustain such localized self-guiding light structures should be nonlinear; their refractive index should be dependent on the light intensity. It has been shown that different types of optical nonlinearities, such as absorptive, dispersive, second-order (quadratic), third-order (cubic, Kerr-like), nonlocal, etc., can be used in practice to prevent either temporal dispersion or spatial diffraction of light beams or both of them. As a result, the field of temporal or spatial optical solitons emerged from these fundamental studies of the interaction of intense laser beams with matter. These temporal/spatial optical solitons could be used as bits of information in both sequential and parallel transmission and processing of information.

However, there also exists a third kind of optical solitons, which are spatially confined pulses of light, the so-called *spatiotemporal optical solitons* [4], alias “light bullets” [6]. These spatiotemporal optical solitons are nondiffracting and nondispersing wavepackets propagating in nonlinear optical media. The three-dimensional (3D) spatiotemporal optical solitons are localized (self-guided) in the two transverse (spatial) dimensions and in the direction of propagation due to the balance of anomalous GVD of the medium in which they form and nonlinear self-phase modulation. Therefore, the “light bullet” is a fully three-dimensional localized object in both space and time. It is now believed that the spatiotemporal optical solitons could be used as information carriers in future all-optical information processing systems due to their remarkable potential for massive parallelism (in space) and pipelining (in time) [4].

However, both two-dimensional (2D) and three-dimensional solitons in self-focusing cubic (Kerr-like) media are unstable because of the occurrence of collapse in the governing nonlinear Schrödinger model [7]. Several possibilities to arrest this intrinsic collapse were considered, such as periodic alternation of self-focusing and defocusing layers [8] and various generalizations of this setting [9], the use of weaker nonlinearities such as saturable nonlinearities [10], quadratic nonlinearities ($\chi^{(2)}$) [11–14], the combination of quadratic and cubic nonlinearities, or self-focusing cubic and self-defocusing quintic nonlinearities [15], the use of tandem layered structures [16], of off-resonance two-level systems [17] and self-induced-transparency media [18].

The undesired collapse effect does not occur in cubic nonlinear media whose optical nonlinearity is nonlocal, therefore these media may also give rise to stable two- and three-dimensional optical solitons, see [19–20]. Moreover, multipole vector solitons in nonlocal nonlinear media [21], one-dimensional solitons of even and odd parities supported by competing nonlocal nonlinearities [22], and 2D vortex solitons [23] and 3D fundamental (vorticityless) and spinning (vortex) solitons [24] were considered in the context of nonlocality in various optical models. Localized optical vortices (alias vortex solitons), have drawn much attention as objects of fundamental interest, and also due to their potential applications to all optical information processing, as well as to the guiding and trapping of atoms [25]. Unique properties are also featured by vortex clusters, such as rotation similar to the vortex motion in superfluids. The complex dynamics of vortex clusters in optical media with competing nonlinearities has been studied too [26]. Various complex patterns based on vortices were theoretically investigated in the usual BEC models, based on the Gross-Pitaevskii equation with the local nonlinearity [27].

Multidimensional soliton necklaces [28–29] and rotating soliton clusters [cite{cluster}] were investigated, too. Moreover, in nondissipative optical media with competing nonlinearities, robust soliton complexes (in the form of “clusters”

or soliton “molecules”) composed by several fundamental (nonspinning) solitons were thoroughly investigated [30]. The quasi-stable propagation of such robust soliton clusters is a generic feature of media with competing nonlinearities (self-focusing cubic and self-defocusing quintic nonlinearities or quadratic nonlinearities in competition with self-defocusing cubic nonlinearities) [30]. A new class of both 2D and 3D spatially modulated vortex solitons, the so-called azimuthons, was introduced recently [31].

Competing combinations of optical nonlinearities such as a combination of quadratic and self-defocusing cubic nonlinearities, or self-focusing cubic and self-defocusing quintic nonlinearities are necessary to prevent the spatiotemporal collapse and they also provide for a possibility to get stable 3D solitons with internal vorticity. Both fundamental (nontopological) and topological (vorticity-carrying) stable three-dimensional spatiotemporal optical solitons have been predicted, in media with such competing optical nonlinearities [15].

It should be mentioned that, while theoretical studies of multidimensional optical solitons have advanced a great deal in recent years, the reported experimental results remain more modest, being thus far limited to the experimental observation of two-dimensional spatiotemporal optical solitons that overcome diffraction in one transverse spatial dimension in quadratic nonlinear optical media [32].

Recently, it was shown the existence of stable three-dimensional spatiotemporal optical solitons confined by either harmonic two-dimensional optical lattices [33] or radially symmetric Bessel lattices [34]. Thus it was predicted the existence of stable three-dimensional spatiotemporal solitons in a two-dimensional photonic lattice and it was found that the Hamiltonian (H)-versus-soliton norm (N) diagram exhibits a generic two-cusp structure. Correspondingly, a “swallowtail” shape of the $H - N$ diagram emerged, which is a quite rare physical phenomenon [33]. This unique feature is a generic one for both nontopological (nonspinning) [33–36] and topological (spinning) [37] 3D solitons. This unique property has been also found in the case of radially symmetric Bessel lattices [34], which is a result suggesting a promising approach to generate both stable „light bullets” in optics and stable three-dimensional solitons in attractive Bose-Einstein condensates [35], and in the search for stable light bullets in media with quadratic nonlinearities in competition with self-focusing cubic nonlinearities [36].

In recent years, there was also an increasing interest in the study of multidimensional dissipative localized structures. These localized physical objects are modeled by nonlinear partial differential equations involving gain and loss terms in addition to the common nonlinear and dispersive/diffractive terms, which allow for the formation under certain conditions of *stable dissipative solitons* [38]. One of the prototype dissipative dynamical system is that governed by the complex Ginzburg-Landau (GL) equation, which is one of the most studied nonlinear partial differential equation in nonlinear science [39]. Recently stable fundamental

(vorticityless) and spinning (with nonzero intrinsic vorticity) spatiotemporal dissipative optical solitons described by the complex cubic-quintic GL equation were found [40–45] and both elastic and inelastic collision scenarios were identified [46–47].

Over the past decades a great deal of interest has been drawn to nonlinear optical surface waves guided by single and multiple interfaces separating different media. Quite often, features exhibited by such *surface optical solitons* have no analogue in the corresponding bulk media, which makes their study especially relevant. The nonlinear surface modes might be potentially useful for practical applications. These electromagnetic waves are a purely nonlinear phenomenon with no counterpart in the linear limit; therefore they exist only if the mode power exceeds a certain threshold. Nonlinear transverse-electric, transverse-magnetic, and mixed polarization surface waves travelling along single and multiple dielectric interfaces were theoretically predicted and systematically analyzed more than two decades ago [48–55]. However, direct observation of surface optical solitons has been hindered by huge experimental difficulties, related to their proper excitation and high power thresholds required for their formation.

Recently, the interest in the study of nonlinear self-trapped optical surface waves has been renewed after the theoretical predictions [56–58] and subsequent experimental demonstrations [59–60] of nonlinearity-induced light localization near the edge of a truncated one-dimensional nonlinear waveguide array that can lead to the formation of the so-called *discrete surface optical solitons*. The generation of discrete surface solitons can be understood with the help of a simple physics [61] as a trapping of the optical field [3] near the repulsive edge of the lattice when the beam power exceeds some threshold value. These surface solitons become possible solely due to discreteness effects and they exist in neither continuous nor linear limits. Some of the specific features of such discrete surface optical solitons in other relevant physical settings have been recently investigated both theoretically [62–65] and experimentally [66–69] (see also Ref. [70] for recent comprehensive overviews of experimental and theoretical developments in the area of discrete optical solitons).

The concept of surface optical solitons has been recently extended to the case of spatiotemporal surface solitons [71–74] described by the continuous-discrete nonlinear equations similar to those investigated earlier for cubic [75] and quadratic [76] nonlinear optical media, but with the properties strongly affected by the presence of the surface in the form of the lattice truncation.

Following our earlier studies [71–74], we recently considered both (2+1)-dimensional [77] and (3+1)-dimensional [78] continuous-discrete spatiotemporal models described by the complex GL equation. We thus investigated the effects of gain and loss due to optical amplifiers and saturable absorbers in truncated periodic photonic structures and we introduced *dissipative surface light bullets* [77, 78]. Similar to other types of discrete dissipative solitons in both one- and two-

dimensional lattices [79–82], the dissipative surface light bullets exhibit novel features that, as a result of both discreteness and gain (loss) effects, have no counterpart in either the continuous limit or in other conservative discrete models for both cubic and quadratic nonlinear media [83–88].

In this work we briefly overview the recent studies of discrete surface spatiotemporal optical solitons (“discrete surface light bullets”). We analyze spatiotemporal light localization near the edges of semi-infinite arrays of weakly coupled nonlinear waveguides and in the corners or at the edges of truncated two-dimensional photonic lattices. We also overview the recent results concerning the existence and stability of the one-dimensional families of discrete surface light bullets and compare the properties of discrete surface spatiotemporal solitons with those of the spatiotemporal nonlinear modes located deep inside the one- and two-dimensional photonic lattices.

2. DISCRETE SURFACE LIGHT BULLETS IN TRUNCATED WAVEGUIDE ARRAYS

Recently we extended the concept of discrete surface solitons and initiated the study of a rich variety of the surface-mediated effects associated with spatiotemporal evolution of surface solitons [71]. We consider a truncated array of weakly coupled nonlinear optical waveguides, which form a one-dimensional photonic lattice, taking into account the spatiotemporal evolution of light near the edge of this semi-infinite waveguide array. Thus we combine the key features of both *continuous* and *discrete* nonlinear models and analyze the existence, stability and robustness of continuous-discrete soliton families describing *discrete surface light bullets*, or in other words, *discrete surface spatiotemporal optical solitons*.

We consider an array of weakly coupled nonlinear optical waveguides described, in the tight-binding approximation, by the effective discrete nonlinear equations [3]. We take into account the spatiotemporal evolution of light, similar to the earlier studies [75], but also assume that our nonlinear waveguide array is truncated so that the spatiotemporal light localization occurs near its edge. The corresponding nonlinear dynamical model can be written in the form,

$$\begin{aligned} i \frac{\partial E_1}{\partial z} - \gamma \frac{\partial^2 E_1}{\partial t^2} + E_2 + \sigma |E_1|^2 E_1 &= 0, \\ i \frac{\partial E_n}{\partial z} - \gamma \frac{\partial^2 E_n}{\partial t^2} + (E_{n+1} + E_{n-1}) + \sigma |E_n|^2 E_n &= 0, \quad n \geq 2, \end{aligned} \tag{1}$$

where $n = 1$ designates the edge of the waveguide array. Here the propagation coordinate z and the dispersion coefficient γ are normalized to the intersite coupling V . In deriving eqs. (1) the actual electric field in the n -th guide \mathbf{E}_n has been decomposed into the product of the vectorial guided mode profile of the

isolated channel waveguide $\mathbf{e}(x, y)$ and the respective mode amplitude ε_n , which can be finally normalized to give $E_n = \sqrt{\chi_{eff} / V} \varepsilon_n$, where the effective nonlinear coefficient is $\chi_{eff} = \frac{\omega}{c} \frac{n_2}{A_{eff}}$. Here n_2 is the nonlinear refractive index of the material and A_{eff} is the effective mode area. The parameter $\sigma = \pm 1$ defines self-focusing or self-defocusing nonlinearities of the waveguide material, respectively.

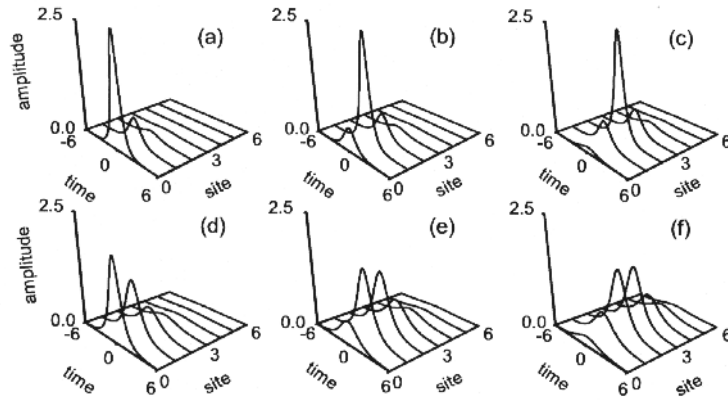


Fig. 1 – Examples of stable discrete surface spatiotemporal optical solitons localized at distances of: a) $d = 0$, b) $d = 1$, and c) $d = 2$ from the edge of the waveguide array (at $\beta = 3.5$), and unstable nonlinear surface modes centered at distances of d) $d = 0$, (e) $d = 1$, and f) $d = 2$ (at $\beta = 2.5$).

The spatiotemporal soliton solutions of this nonlinear dynamical model are looked for in the form $E_n(t; z) = \exp(i\beta z) E_n(t)$, where β is the nonlinearity-induced shift of the waveguide propagation constant, serving likewise as a family parameter, and the envelope $E_n(t)$ describes the temporal evolution of the soliton-like pulse in the n -th waveguide. We consider here only the case of anomalous dispersion ($\gamma < 0$), self-focusing nonlinearity ($\sigma = +1$) *in-phase solitons* (unstaggered solutions).

We can scale out the dispersion parameter by the transformation $t \rightarrow \tau \sqrt{|\gamma|}$ and we obtain

$$\begin{aligned} \frac{dE_1}{d\tau^2} - \beta E_1 + E_2 + |E_1|^2 E_1 &= 0, \\ \frac{d^2 E_n}{d\tau^2} - \beta E_n + (E_{n+1} + E_{n-1}) + |E_n|^2 E_n &= 0, \quad n \geq 2, \end{aligned} \quad (2)$$

We found numerically localized solutions $E_n(\tau)$ of the coupled equations (2) assuming that the amplitude of the pulses in each waveguide, $\max|E_n|$, decays rapidly far from the edge of the waveguide array, so that the corresponding solution describes a mode localized near the surface [71].

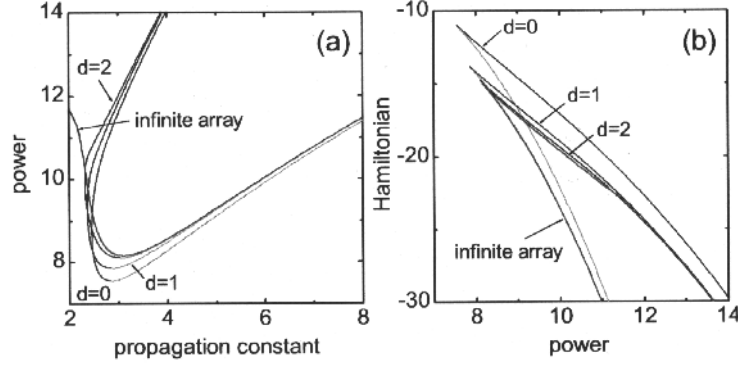


Fig. 2 – Families of discrete surface light bullets: a) normalized power versus propagation constant β for the surface solitons located at the distances $d = 0$, $d = 1$, and $d = 2$ from the edge of the waveguide array; b) Hamiltonian *versus* power for the localized nonlinear surface modes.

Figure 1 shows several examples of stable [panels (a), (b), and (c)] and unstable [panels (d), (e), and (f)] nonlinear spatiotemporal continuous-discrete localized states ('discrete surface light bullets') located at different distances d from the edge of the one-dimensional photonic lattice. The nonlinear modes can be characterized by the total mode power

$$P(\beta) = \sum_{n=1}^{\infty} \int_{-\infty}^{+\infty} |E_n(\beta)|^2 d\tau, \quad (3)$$

which is a conserved quantity.

The solution centered at $n = 1$ (that is, at the distance $d = 0$ from the edge of the waveguide array) describes the light bullet with the maximum localized at the edge of the semi-infinite waveguide array; this solution is a spatiotemporal generalization of the discrete surface solitons predicted earlier in Ref. [57]. The typical field distribution of other surface spatiotemporal nonlinear modes are shown in Figs. 1(b)-(f), with the corresponding power dependencies constructed in Fig. 2(a); they describe the crossover regime between the continuous-discrete surface light bullet of Fig. 1(a), with the maximum amplitude located at the surface, and their counterpart predicted to exist deep inside of the waveguide arrays [75] when the surface effects vanish. If we compare the corresponding power curves of different surface modes including the case of a spatiotemporal soliton localized deep inside the array [see the curve corresponding to infinite

arrays in Fig. 2(a)], we notice that the threshold power of surface localized modes is lower than that of the bulk mode. Therefore, in sharp contrast with one-dimensional surface solitons [57, 61], the edge of a semi-infinite waveguide array creates an effectively attractive potential for the spatiotemporal localized modes that reduces the threshold power for the nonlinear mode localization at the surface.

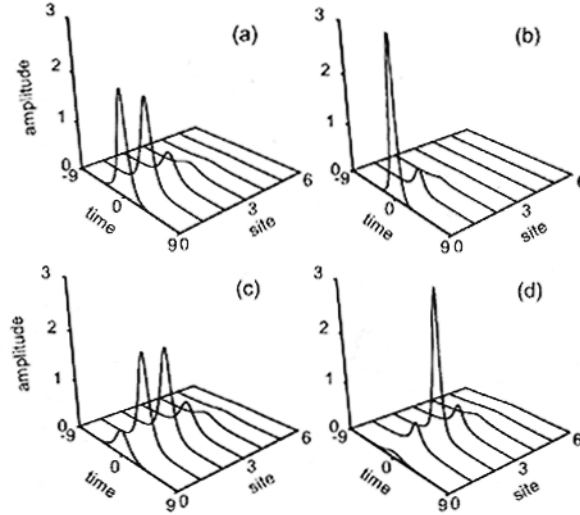


Fig. 3 – Instability-driven evolution of unstable solitons corresponding to the upper branches in Fig. 2 for $\beta = 3$: a,b) reshaping of the unstable $d = 0$ soliton ($z = 0$) into a stable $d = 0$ soliton at $z = 1200$; c,d) hopping of the unstable $d = 1$ soliton ($z = 0$) into the neighboring site and the generation of a stable $d = 2$ soliton at $z = 1200$.

To analyze the linear stability of each nonlinear surface mode found numerically, we need to calculate not only the mode power (3) but also the second conserved quantity of the dynamical system (1), that is, the Hamiltonian H of the corresponding conservative dynamical system [71]. We thus expect that the *stable* surface spatiotemporal optical solitons should correspond to the lower branch of the dependence $H = H(P)$. The occurrence of the typical single cusp of the curve $H = H(P)$ is shown in Fig. 2(b). The upper branches of the Hamiltonian-power curves correspond to unstable surface solitons, whereas the lower branches correspond to stable surface modes. This conclusion is fully confirmed by direct numerical simulations of the propagation of the stationary surface solitons perturbed by a white input noise.

Figures 3(a-d) demonstrate two different scenarios of the evolution of unstable high-power spatiotemporal solitons located at the distances $d = 0$ and $d = 1$ from the edge of the waveguide array and corresponding to the upper unstable branches in Figs. 2(a) and 2(b). Typically, we observe either reshaping of an unstable soliton into a stable soliton of the same family [see Fig. 3(a,b)] or

hopping of the surface mode into the neighboring site and the formation of a stable soliton pertaining to another family with the center position shifted away from the surface [see Figs. 3(c,d)].

The results briefly overviewed here can be easily extended for describing spatiotemporal localization effects for staggered solitons (π -out of phase nonlinear modes) such as *surface gap solitons* [58–60] in self-defocusing nonlinear optical media with normal GVD.

As concerning the implementation of the results presented in this section to a concrete physical setting we mention that recently the conditions for low-power spatiotemporal soliton formation in arrays of evanescently-coupled silicon-on-insulator (SOI) photonic nanowires have been thoroughly analyzed [85]. It was shown in Ref. [85] that pronounced soliton effects can be observed even in the presence of realistic loss, two-photon absorption, and higher-order GVD. The well established SOI technology offers an exciting opportunity in the area of spatiotemporal optical solitons because a strong anomalous GVD can be achieved with nanoscaled transverse dimensions and moreover, the enhanced nonlinear response resulting from this tight transverse spatial confinement of the electromagnetic field leads to soliton peak powers of only a few watts for 100-fs pulse widths (the corresponding energy being only a few hundreds fJ). The arrays of SOI photonic nanowires seem to be suitable for the observation of discrete surface light bullets because a suitable design of nanowires can provide dispersion lengths in the range of 1 mm and coupling lengths of a few millimeters (for 100-fs pulse durations) [85].

3. INTERFACE DISCRETE LIGHT BULLETS IN WAVEGUIDE ARRAY

Next we analyze spatiotemporal light localization at the interface separating two different periodic one-dimensional photonic lattices, that is, two different arrays of optical waveguides. We demonstrate the existence of a novel class of continuous-discrete spatiotemporal solitons propagating along the interface, including *hybrid staggered-unstaggered discrete light bullets* with tails belonging to the spectral gaps of different types.

We consider light propagation in an inhomogeneous array of optical waveguides described by the system of coupled-mode equations [3], where we take into account the spatiotemporal evolution of light, similar to the earlier studies [75]. The corresponding nonlinear system of coupled equations can be written in the form,

$$i \frac{\partial E_n}{\partial z} - \gamma_n \frac{\partial^2 E_n}{\partial t^2} + (E_{n+1} + E_{n-1}) + f_n |E_n|^2 E_n = 0, \quad (4)$$

where $f_n(|E_n|^2) = \varepsilon_n + \sigma_n |E_n|^2$, the propagation coordinate z and dispersion coefficient γ_n are normalized to the intersite coupling V (see also the preceding section).

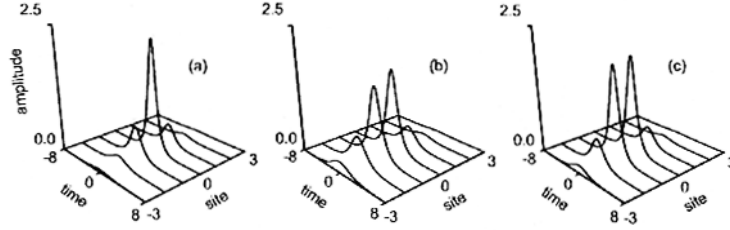


Fig. 4 – Examples of (a) stable (at $\beta = 3.7$) and (b), (c) unstable (at $\beta = 3.2$ and $\beta = 3.7$, respectively) unstaggered (in-phase) spatiotemporal interface light bullets.

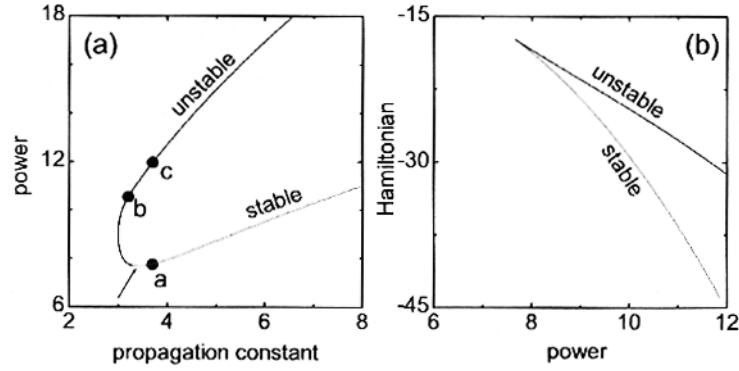


Fig. 5 – Families of unstaggered spatiotemporal interface solitons. (a) Power versus propagation constant. Points a-c mark the modes shown in Figs. 4(a)-4(c), respectively. (b) Hamiltonian versus power.

We then consider two semi-infinite waveguide arrays described by Eq. (4) with different propagation constants ε_A , and ε_B , with $n = 0$ being an interface site. We define $\varepsilon_n = \varepsilon_A$ for $n < 0$, $\varepsilon_n = \varepsilon_0$ at $n = 0$, and $\varepsilon_n = \varepsilon_B$ for $n > 0$. We focus on the interface localized modes defined by having their centers at either the first of the A waveguides or the first of the B waveguides, and also consider different combinations of the normalized dispersion ($\gamma_n = \pm 1$) and nonlinearity ($\sigma_n = \pm 1$). As in the previous section we look for spatiotemporal localized modes in the form $E_n(t; z) = \exp(i\beta z)E_n(t)$, where β is the nonlinearity-induced shift of the propagation constant serving likewise as a family parameter, and the envelope

$E_n(t)$ describes the temporal evolution of the solitonlike pulse in the n -th waveguide. We find numerically localized solutions $E_n(t)$ of the above coupled nonlinear equations, assuming that the amplitude of the pulse in each waveguide, $\max|E_n|$, decays rapidly far from the interface, so that the corresponding solution describes a localized mode.

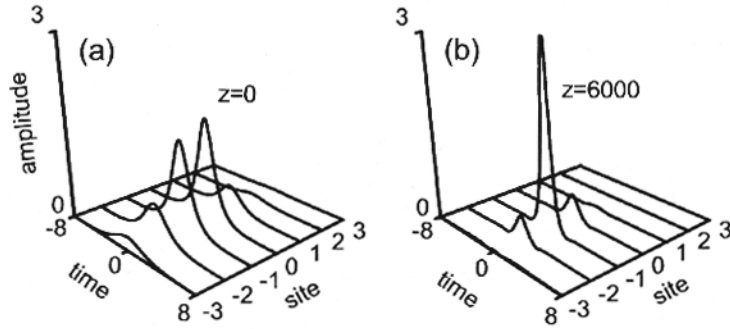


Fig. 6 – Hopping of the unstable (at $\beta = 3.2$) soliton centered at $n=0$ into the neighboring site $n = -1$.

Figures 4(a)-4(c) show several examples of the unstaggered spatiotemporal continuous-discrete nonlinear states located at the interface $n = 0$ for $\varepsilon_A = \varepsilon_0 = -\varepsilon_B = 0.6$, and the focusing nonlinearity ($\sigma_n = +1$); these modes generalize the continuous-wave discrete interface modes analyzed earlier [89, 90] in the case of the interface pulse propagation for the anomalous GVD ($\gamma_n = -1$).

To analyze the linear stability of each nonlinear state found numerically, we calculate the total mode power $P = P(\beta)$ [see Fig. 5(a) where the arrow marks the point separating stable and unstable branches of the dependence $P = P(\beta)$]. The typical single-cusp behavior of the dependence $H = H(P)$ is shown in Fig. 5(b) where the lower branch corresponds to the stable interface modes. The predictions of the mode stability gained from the (H, P) diagram have been confirmed by both linear stability analysis and direct simulations of the propagation of the stationary solitons perturbed by a white input noise. We have found different scenarios of the evolution of unstable spatiotemporal solitons corresponding to the upper unstable branches in Figs. 5(a) and 5(b). Figures 6(a) and 6(b) show a typical example of mode hopping into the neighboring site and the formation of a stable light bullet with the center position shifted away from the interface. It is worthy to notice that in sharp contrast with the discrete spatial interface modes [89, 90], the spatiotemporal hybrid staggered-unstaggered interface solitons (with tails belonging to spectral gaps of different types) may appear in a very narrow parameter domain and under special conditions [72].

4. DISCRETE SURFACE LIGHT BULLETS IN TRUNCATED BINARY WAVEGUIDE ARRAYS

In this section we study spatiotemporal optical solitons at the edge of a semi-infinite binary array of optical waveguides and, in particular, we predict theoretically the existence of a novel type of surface soliton, the *surface gap light bullets*. We then analyze the stability properties of these solitons in the framework of the continuous-discrete model of arrays of two types of optical waveguides.

We next describe the unique features of discrete surface spatiotemporal optical solitons in binary waveguide arrays. In the tight-binding approximation, the model of the binary waveguide array is known to support two different types of discrete optical solitons localized either in the total internal reflection (TIR) gap or in the Bragg-reflection (BR) gaps. These solitons have been previously analyzed theoretically [91] and then observed experimentally [92]. Here we consider two different types of truncated binary waveguide arrays taking into account the spatiotemporal evolution of light near the edge of the waveguide array. We thus combine the key features of both continuous and discrete nonlinear models and analyze the existence and stability of continuous-discrete soliton families describing spatiotemporal discrete surface light bullets in binary waveguide arrays.

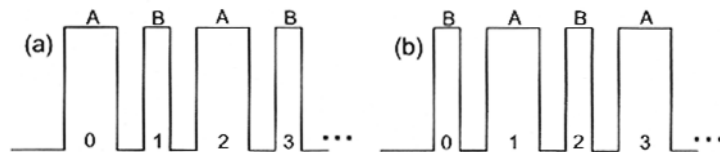


Fig. 7 – Schematic structure of a binary array of weakly coupled optical waveguides truncated at: a) wide and b) narrow waveguides, respectively.

We consider spatiotemporal light localization in a semi-infinite periodic binary array of alternating wide and narrow weakly coupled optical waveguides, as shown schematically in Figs. 7. As was established earlier [91, 92] for infinite binary waveguide arrays, the properties of spatial discrete solitons can be effectively managed by controlling the geometry of the waveguide arrays, e.g., the intrinsic parameters of two types of semi-infinite (truncated) arrays.

We next describe the binary array in the framework of the tight-binding approximation where the total field is decomposed into a superposition of weakly overlapping modes of individual waveguides of two kinds [A (wide waveguide) and B (narrow waveguide)]. We take into account the spatiotemporal evolution of light, similar to the earlier studies [75], but also assume that our waveguide array is

truncated so that the light localization occurs near its edge (see Fig. 7). The corresponding governing equations for the mode amplitudes take the form,

$$i \frac{\partial E_n}{\partial z} - \gamma_n \frac{\partial^2 E_n}{\partial t^2} + (E_{n+1} + E_{n-1}) + f_n |E_n|^2 E_n = 0, \quad (5)$$

where $f_n(|E_n|^2) = \rho_n + \sigma_n |E_n|^2$. Here $n = 0, 1, \dots$, and $E_{-1} \equiv 0$ due to the layered structure termination. The parameter γ_n is the GVD coefficient, ρ_n characterizes the linear propagation constant of the mode guided by the n -th waveguide, and σ_n are the effective nonlinear coefficients. For the structure shown in Fig. 7(a), i.e., for a binary array truncated at the wide waveguide, we take $\rho_{2n} = \rho$, and $\rho_{2n+1} = -\rho$, whereas for the structure shown in Fig. 7(b), i.e., for a binary array truncated at the narrow waveguide, we have $\rho_{2n} = -\rho$ and $\rho_{2n+1} = \rho$. We consider also $\sigma_n = -\gamma_n = -\text{sign}(\rho_n)$, for all n . In the numerical simulations outlined below we take $\rho = 0.6$ and also consider both types of nonlinearity, i.e., $\sigma_n = \pm 1$.

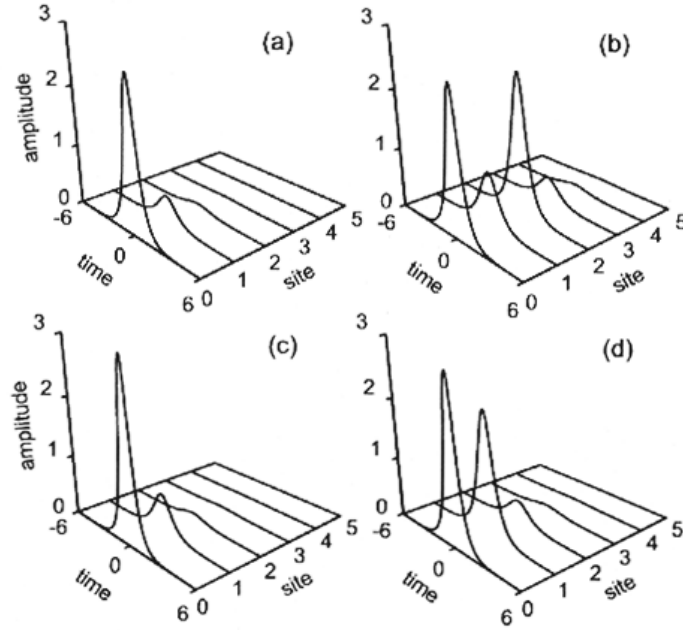


Fig. 8 – Examples of unstaggered spatiotemporal solitons corresponding to points a-d in Fig. 9, for $\beta = 4$: a) stable and b) unstable discrete surface light bullets in the array truncated at the wide waveguide; c) stable and d) unstable surface solitons in the array truncated at the narrow waveguide.

Figures 8(a)-8(d) show several examples of both stable and unstable nonlinear spatiotemporal continuous-discrete localized states ('discrete surface light bullets') located near the edges of the two kinds of binary waveguide arrays for the case of self-focusing nonlinearity ($\sigma=1$). Examples of unstaggered (in-phase) spatiotemporal solitons plotted in Fig. 8 correspond to points a–d in Fig. 9(a) and are found at $\beta = 4$. It is expected that stable spatiotemporal solitons should correspond to the lower branch of the dependence $H = H(P)$ [see Fig. 9(b), where the typical single-cusp behavior of the dependence $H = H(P)$ is shown]. The arrows in Fig. 9(a) mark the points separating stable and unstable branches. Direct numerical simulations of the propagation of the stationary solitons perturbed by a white input noise confirm this expectation [73]. Moreover, by direct numerical simulations, we have found that the interface ($n = 0$) unstable solitons reshape to stable solitons located on the same site, pertaining to the lower (stable) branch of the soliton family.

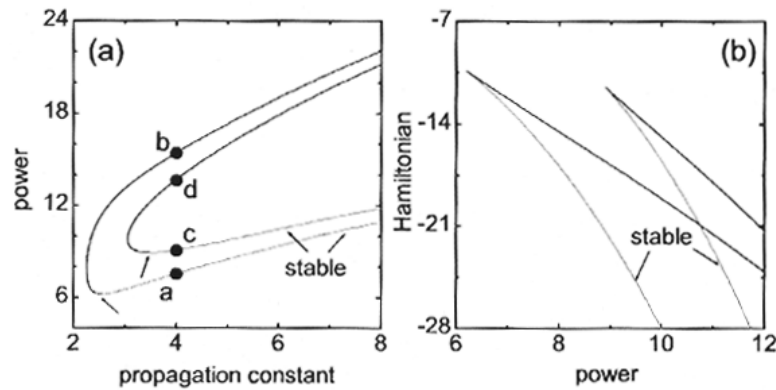


Fig. 9 – Families of discrete unstaggered surface light bullets in the binary array truncated at the wide waveguide (first curve from the left in both panels), and in the waveguide array truncated at the narrow waveguide (second curve from the left in both panels); a) power *versus* propagation constant. Points a–d mark the modes shown in Figs. 8(a)-8(d), respectively; b) Hamiltonian *versus* power.

The linear spectrum of the binary waveguide array consists of two different bands separated by a gap which occurs due to the difference between two types of waveguides A and B. The spatiotemporal discrete surface solitons studied above are located in the TIR gap, and they have unstaggered field profiles. A novel type of spatial solitons, *gap solitons*, appears in the spectral gap due to the Bragg reflection [91]. Therefore, surface spatiotemporal optical solitons in the BR gap can also exist [73], and they can naturally be termed as *surface gap light bullets*; such solitons should have staggered field profiles, and they can be associated with

the surface Tamm states, similar to the case of waveguide arrays with self-defocusing nonlinearity [58, 60].

In conclusion, in the study of spatiotemporal light localization at the edge of semi-infinite binary waveguide arrays, we have revealed the existence of two different classes of discrete surface spatiotemporal optical solitons including a novel class of discrete surface gap light bullets which can be regarded as a generalization of the familiar surface Tamm states to the spatiotemporal domain.

5. DISCRETE SURFACE LIGHT BULLETS IN TWO-DIMENSIONAL PHOTONIC LATTICES

Theoretical studies of discrete surface spatial solitons localized in the corners or at the edges of two-dimensional photonic lattices [93–95] and recent experimental observations of two-dimensional surface spatial solitons in optically-induced photonic lattices [96] and laser-written waveguide arrays in fused silica [97] demonstrated novel features of these nonlinear surface modes in comparison with their counterparts in one-dimensional waveguide arrays [57, 59, 61]. In particular, in a sharp contrast to one-dimensional discrete surface spatial solitons, the nonlinear mode threshold is lower at the surface than in a bulk making the mode excitation easier [94].

In this section we briefly overview the results concerning spatiotemporal light localization in truncated two-dimensional photonic lattices and demonstrate the existence of discrete surface light bullets localized in the lattice corners or the edges [74]. We get the one-parameter families of discrete spatiotemporal surface solitons, study their stability and compare their unique properties with those of the nonlinear modes located deep inside the two-dimensional photonic lattice.

We consider a truncated two-dimensional photonic lattice described by the coupled-mode equations for the normalized amplitudes $E_{n,m}$ of the electric field,

$$i \frac{\partial E_{n,m}}{\partial z} - \gamma \frac{\partial^2 E_{n,m}}{\partial t^2} + \left(V_n + V_m + \sigma |E_{n,m}|^2 \right) E_{n,m} = 0, \quad (6)$$

where z is the normalized propagation distance, the lattice indices are $n, m = 0, 1, \dots$, and $E_{-1,m} = E_{n,-1} \equiv 0$ due to the lattice termination [see Figs. 10(a)-(c)]. Here γ is the dispersion coefficient, and $\sigma = \pm 1$ is for either self-focusing or self-defocusing nonlinearity. We define the lattice couplings as: $V_n E_{n,m} = E_{1,m}$, for $n = 0, m \geq 0$ and $V_n E_{n,m} = E_{n+1,m} + E_{n-1,m}$, for $n > 0$, respectively $V_m E_{n,m} = E_{n,1}$ for $m = 0, n \geq 0$ and $V_m E_{n,m} = E_{n,m+1} + E_{n,m-1}$, for $m > 0$.

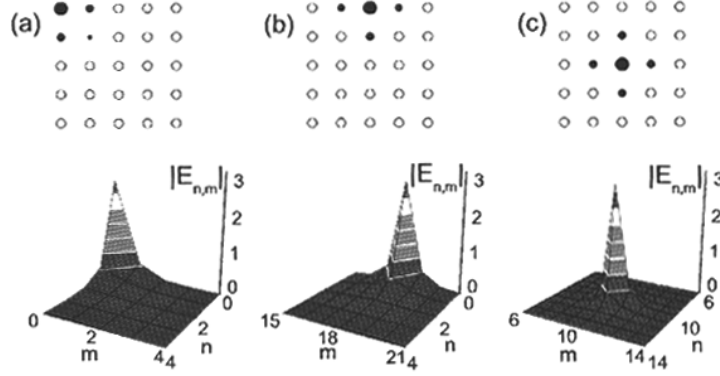


Fig. 10 – a–c) Examples of the modes localized (top) in the lattice corner, at the edge, and in the center of the lattice. Spatial cross sections (bottoms) of the corresponding stable spatiotemporal surface solitons. The modes correspond to points (a)–(c) in Fig. 12(c) for: (a) $\beta = 5$, $\mathcal{E} = 9.5$; b) $\beta = 5.5$, $\mathcal{E} = 10.09$; and c) $\beta = 6$, $\mathcal{E} = 10.66$.

We are looking for spatiotemporal soliton solutions of this nonlinear model in the form $E_{n,m}(t; z) = E_{n,m}(t) \exp(i\beta z)$, where β is the nonlinearity-induced shift of the propagation constant (soliton family parameter), and the envelope $E_{n,m}(t)$ describes the temporal shape of the soliton-like pulse at the (n, m) lattice site. We find different one-parameter families of localized surface solitons by solving the stationary version of Eqs. (6) by means of a standard band-matrix algorithm applied to the corresponding two-point boundary-value problem [74],

$$\gamma \frac{d^2 E_{n,m}}{dt^2} + \left(-\beta + V_n + V_m + \sigma |E_{n,m}|^2 \right) E_{n,m}. \quad (7)$$

The solutions of the above coupled differential equations become less localized near the minimum (cut-off) value of the propagation constant ($\beta_{co} = 4$). Therefore, depending on the value of the propagation constant, we have used up to 301 discretization points in the continuous time interval $[0, t_{\max}]$, and up to 35×35 grid points for the discrete spatial coordinates [74]. Figures 10 and 11 present several typical examples of spatiotemporal continuous-discrete localized states (discrete surface light bullets) located in the corners or at the edges of the two-dimensional photonic lattice, together with the central nonlinear mode representing a discrete spatiotemporal optical soliton in an infinite two-dimensional photonic lattice, for the self-focusing nonlinearity ($\sigma = +1$).

To make a preliminary conclusion about the linear stability of the surface states found numerically, we calculate the total mode energy and the Hamiltonian $H = H(\mathcal{E})$ of the corresponding conservative dynamical system (see Fig. 12 (b)).

$$\mathcal{E}(\beta) = \sum_{n,m} \int_{-\infty}^{+\infty} |E_{n,m}(\beta)|^2 dt, \quad (8)$$

$$H = -\sum_{n,m} \int_{-\infty}^{+\infty} \left\{ \left[E_{n,m} (E_{n+1,m}^* + E_{n,m+1}^*) + c.c. \right] + \gamma \left| \frac{\partial E_{n,m}}{\partial t} \right|^2 + \frac{1}{2} \sigma |E_{n,m}|^4 \right\} dt.$$

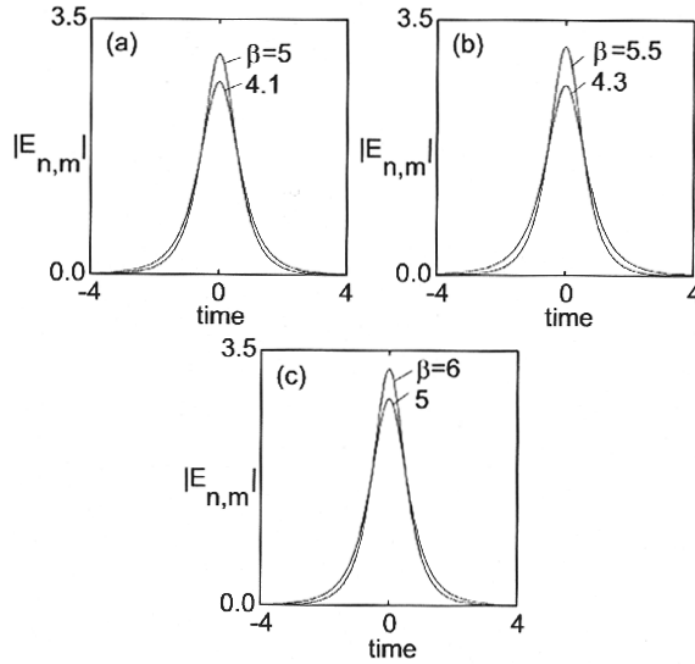


Fig. 11 – Temporal cross sections of spatiotemporal surface solitons localized in the corner, at the edge, and in the center of the lattice, respectively. Shown are the profiles of stable (higher curves) and unstable (lower curves) spatiotemporal solitons corresponding to points (a)-(f) in Fig. 12(c).

Figures 12(a)-(c) present several one-parameter families of spatiotemporal continuous-discrete surface solitons found numerically for the modes localized in the corner, at the edge, and in the center of the two-dimensional photonic lattice. The one-parameter families are characterized by the dependencies $\mathcal{E} = \mathcal{E}(\beta)$ and $H = H(\mathcal{E})$, as well as the dependence of the peak amplitude $\max |E_{n,m}|$ on the total energy. We expect that stable spatiotemporal solitons should correspond to the lower branch of the dependence $H = H(\mathcal{E})$. The typical single-cusp behavior of the dependence $H = H(\mathcal{E})$ is shown in Fig. 12(b) where the lower branches

correspond to the stable surface nonlinear modes. This observation is fully confirmed by direct numerical simulations of the propagation of the stationary solitons perturbed by a white input noise (see below).

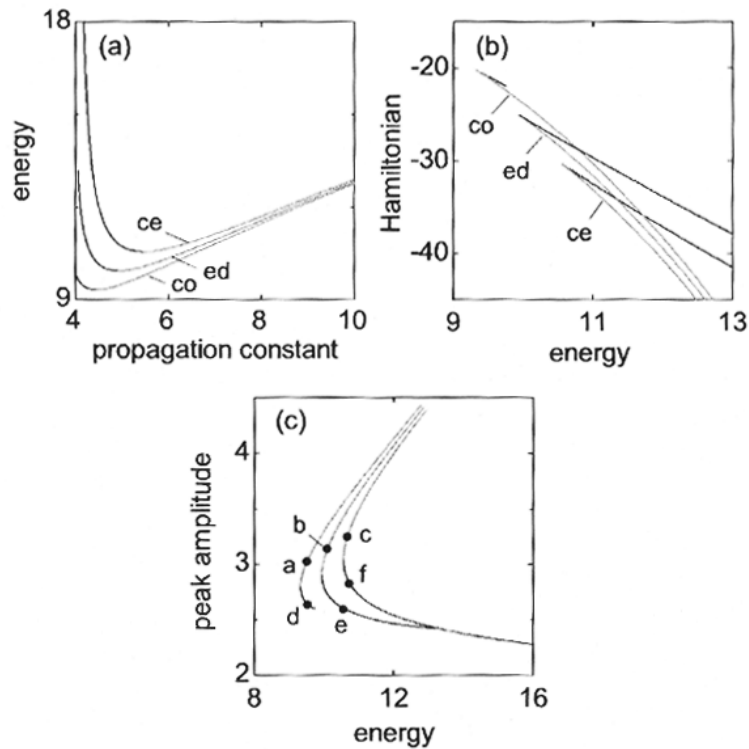


Fig. 12 – Families of spatiotemporal surface solitons in two-dimensional lattices for the modes localized in the corner (co), at the edge (ed), and in the center (ce), respectively: a) power versus propagation constant; b) Hamiltonian versus power; c) peak amplitude versus power. Points (a)-(f) mark the examples shown in Figs. 10 and 11.

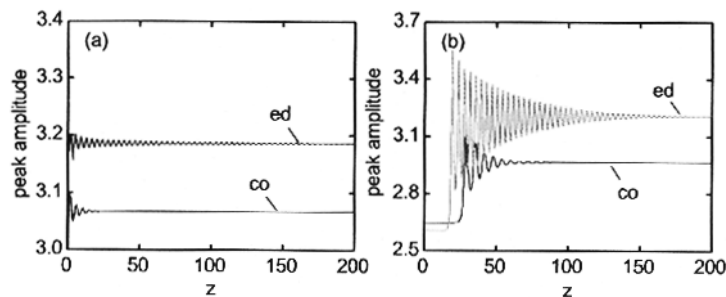


Fig. 13 – Evolution of the soliton amplitude versus propagation distance for a) stable corner (co) ($\beta = 5.0$), and edge (ed) ($\beta = 5.5$) spatiotemporal surface solitons perturbed by a white input noise, and b) unstable, unperturbed corner (co) ($\beta = 4.1$) and edge (ed) ($\beta = 4.3$) spatiotemporal surface solitons.

Figure 12(c) shows the energy dependence of the peak amplitude of stationary spatiotemporal solitons. As expected, for a fixed energy there exist two stationary solitons, stable and unstable ones, the stable soliton having the peak amplitude larger than the unstable one and, correspondingly, a smaller width. The threshold energy \mathcal{E}_{th} for the spatiotemporal surface soliton generated in a two-dimensional photonic lattice is smaller than that corresponding to the spatiotemporal soliton located far away from the lattice edges, with the corner surface soliton having the smallest threshold energy: $\mathcal{E}_{th} = 9.317$ (corner), $\mathcal{E}_{th} = 9.933$ (edge), and $\mathcal{E}_{th} = 10.553$ (central). This conclusion is similar to the case of two-dimensional discrete spatial solitons, see Refs. [89, 94]. These numerical results should be compared to the value of the threshold power of discrete surface light bullets in one-dimensional photonic lattices [71]: $P_{th} \approx 7.55$. The stability results following directly from the analysis of the dependence $H = H(\mathcal{E})$ shown in Fig. 12(b), have been cross-checked by direct numerical simulations of the dynamic equations (6) carried out by means of the Crank-Nicholson scheme; transparent boundary conditions were implemented in order to permit the escape of radiation from the computation window [74]. The results of the direct propagation simulations are found to be in agreement with the predictions of the (H, \mathcal{E}) diagram. Thus, we find that stable spatiotemporal surface solitons resist a 10% input white noise, see Fig. 13(a), whereas unstable solitons reshape and transform into stable solitons pertaining to the lower (stable) branch of the soliton family, by increasing their peak amplitude during this process, as shown in Fig. 13(b).

In conclusion, we have demonstrated that the properties of such continuous-discrete localized surface states in two-dimensional photonic lattices are similar to those of spatiotemporal solitons localized far away from the lattice edges, and they differ substantially from the properties of one-dimensional discrete surface spatial solitons [57, 61].

6. CONCLUSIONS

In this work we overviewed some recent results concerning the existence, stability and robustness of discrete surface spatiotemporal optical solitons (“discrete surface light bullets”). We analyzed spatiotemporal light localization near the edges of semi-infinite arrays of weakly coupled nonlinear waveguides and in the corners or at the edges of truncated two-dimensional photonic lattices and demonstrated the existence of novel classes of continuous-discrete spatiotemporal optical solitons. We also analyzed the spatiotemporal light localization at the interface separating two different waveguide arrays and at the edges of semi-

infinite binary waveguide arrays. We studied these one-parameter families of discrete surface light bullets and compared their unique features with those of the spatiotemporal nonlinear modes located deep inside the photonic lattices.

Once stable discrete surface light bullets are available, a problem of great interest is to consider collisions between them. Recently [98] we presented generic outcomes of collisions between discrete surface spatiotemporal solitons in nonlinear waveguide arrays and we studied the effects associated with the spatiotemporal light localization near the edge of semi-infinite arrays of weakly coupled nonlinear optical waveguides. We demonstrated that the collision outcomes were strongly affected by the presence of the surface and we shown that they depend on the initial surface soliton parameters, such as the distance of their centers from the surface and their transverse velocities. In addition to well-known scenarios of soliton fusion and symmetric scattering, we have observed strongly asymmetric collision outcomes [98]. An equally interesting open problem is the extension of these results to the case of discrete surface light bullets in two-dimensional photonic lattices.

Acknowledgements. Part of the research work overviewed in this paper has been carried out in collaboration with Falk Lederer and Yuri S. Kivshar. We are deeply indebted to them.

REFERENCES

1. N. N. Akhmediev, A. Ankiewicz, *Solitons: Nonlinear Pulses and Beams*, London, Chapman and Hall, 1997.
2. G. I. Stegeman, D. N. Christodoulides, M. Segev, *IEEE J. Select. Top. Quant. Electron.*, **6**, 1419 (2000).
3. Y. S. Kivshar, G. P. Agrawal, *Optical solitons: From fibers to photonic crystals*, Academic Press, San Diego, 2003.
4. B. A. Malomed, D. Mihalache, F. Wise, L. Torner, *J. Opt. B: Quantum Semiclassical Opt.*, **7**, R53 (2005).
5. D. Mihalache, D. Mazilu, *Rom. Rep. Phys.*, **60**, 957 (2008).
6. Y. Silberberg, *Opt. Lett.*, **15**, 1282 (1990).
7. L. Bergé, *Phys. Rep.*, **303**, 260 (1998);
V. V. Konotop, P. Pacciani, *Phys. Rev. Lett.*, **94**, 240405 (2005).
8. I. Towers, B. A. Malomed, *J. Opt. Soc. Am. B*, **19**, 537 (2002).
9. B. A. Malomed, *Soliton Management in Periodic Systems*, Springer, New York, 2006.
10. D. Edmundson, R. H. Enns, *Opt. Lett.*, **17**, 586 (1992);
N. Akhmediev, J. M. Soto-Crespo, *Phys. Rev. A*, **47**, 1358 (1993);
R. McLeod, K. Wagner, S. Blair, *Phys. Rev. A*, **52**, 3254 (1995).
11. B. A. Malomed *et al.*, *Phys. Rev. E*, **56**, 4725 (1997).
12. D. V. Skryabin, W.J. Firth, *Opt. Commun.*, **148**, 79 (1998).
13. L. Torner, D. Mazilu, D. Mihalache, *Phys. Rev. Lett.*, **77**, 2455 (1996);
D. Mihalache, F. Lederer, D. Mazilu, L.-C. Crasovan, *Opt. Eng.*, **35**, 1616 (1996);

- D. Mihalache, D. Mazilu, L.-C. Crasovan, L. Torner, *Opt. Commun.*, **137**, 113 (1997);
D. Mihalache *et al.*, *Phys. Rev. E*, **62**, R1505 (2000).
14. D. Mihalache *et al.*, *Opt. Commun.*, **152**, 365 (1998); *Opt. Commun.*, **169**, 341 (1999); *Opt. Commun.*, **159**, 129 (1999); *Phys. Rev. E*, **62**, 7340 (2000);
N.-C. Panoiu *et al.*, *Phys. Rev. E*, **71**, 036615 (2005).
15. D. Mihalache *et al.*, *Phys. Rev. Lett.*, **88**, 073902 (2002); D. Mihalache *et al.*, *Phys. Rev. E*, **66**, 016613 (2002);
H. Michinel, M. J. Paz-Alonso, V. M. Perez-Garcia, *Phys. Rev. Lett.*, **96**, 023903 (2006);
D. Mihalache, D. Mazilu, L.-C. Crasovan, B. A. Malomed, F. Lederer, *Phys. Rev. E*, **61**, 7142 (2000);
A. Desyatnikov, A. Maimistov, B. Malomed, *Phys. Rev. E*, **61**, 3107 (2000).
16. L. Torner *et al.*, *Opt. Commun.*, **199**, 277 (2001).
17. I. V. Mel'nikov, D. Mihalache, N.-C. Panoiu, *Opt. Commun.*, **181**, 345 (2000).
18. M. Blaauw, B. A. Malomed, G. Kurizki, *Phys. Rev. Lett.*, **84**, 1906 (2000).
19. W. Krolikowski, O. Bang, *Phys. Rev. E*, **63**, 016610 (2001);
M. Peccianti, C. Conti, and G. Assanto, *Phys. Rev. E*, **68**, 025602 (2003);
W. Krolikowski *et al.*, *J. Opt. B: Quantum Semiclass. Opt.*, **6**, S288 (2004).
20. D. Mihalache, *Rom. Rep. Phys.*, **59**, 515 (2007).
21. Y. V. Kartashov, L. Torner, V. A. Vysloukh, D. Mihalache, *Opt. Lett.*, **31**, 1483 (2006).
22. D. Mihalache *et al.*, *Phys. Rev. E*, **74**, 066614 (2006).
23. D. Briedis *et al.*, *Opt. Express*, **13**, 435 (2005);
A. I. Yakimenko, Y. A. Zaliznyak, Y. Kivshar, *Phys. Rev. E*, **71**, 065603 (2005);
A. I. Yakimenko, V. M. Lashkin, O. O. Prikhodko, *Phys. Rev. E*, **73**, 066605 (2006);
V. M. Lashkin, *Phys. Rev. A*, **75**, 043607 (2007).
24. D. Mihalache *et al.*, *Phys. Rev. E*, **73**, 025601 (2006);
Yu. A. Zaliznyak, A. I. Yakimenko, *Phys. Lett. A*, **372**, 2862 (2008).
25. D. Rozas, Z. S. Sacks, G. A. Swartzlander, *Phys. Rev. Lett.*, **79**, 3399 (1997).
26. D. Mihalache *et al.*, *Phys. Rev. E*, **67**, 056608 (2003);
D. Mihalache *et al.*, *J. Opt. B: Quantum Semiclassical Opt.*, **6**, S341 (2004);
M. J. Paz-Alonso, H. Michinel, *Phys. Rev. Lett.*, **94**, 093901 (2005).
27. L.-C. Crasovan *et al.*, *Phys. Rev. E*, **66**, 036612 (2002); *Phys. Rev. A*, **68**, 063609 (2003);
T. Mizushima, N. Kobayashi, K. Machida, *Phys. Rev. A*, **70**, 043613 (2004);
M. Mottonen, S. M. M. Virtanen, T. Isoshima, M. M. Salomaa, *Phys. Rev. A*, **71**, 033626 (2005).
28. M. Soljacic, S. Sears, M. Segev, *Phys. Rev. Lett.*, **81**, 4851 (1998);
A. S. Desyatnikov, Y. S. Kivshar, *Phys. Rev. Lett.*, **87**, 033901 (2001).
29. Y. J. He, H. H. Fan, J. W. Dong, H. Z. Wang, *Phys. Rev. E*, **74**, 016611 (2006);
Y. J. He, B. A. Malomed, H. Z. Wang, *Opt. Express*, **15**, 17502 (2007);
Y. J. He, B. A. Malomed, D. Mihalache, H. Z. Wang, *Phys. Rev. A*, **77**, 043826 (2008).
30. A. S. Desyatnikov, Y. S. Kivshar, *Phys. Rev. Lett.*, **88**, 053901 (2002);
Y. V. Kartashov *et al.*, *Phys. Rev. Lett.*, **89**, 273902 (2002);
L.-C. Crasovan *et al.*, *Phys. Rev. E*, **67**, 046610 (2003);
D. Mihalache *et al.*, *Phys. Rev. E*, **68**, 046612 (2003);
D. Mihalache *et al.*, *J. Opt. B: Quantum Semiclassical Opt.*, **6**, S333 (2004).
31. A. S. Desyatnikov, A. A. Sukhorukov, Yu. S. Kivshar, *Phys. Rev. Lett.*, **95**, 203904 (2005);
V. M. Lashkin, A. I. Yakimenko, O. O. Prikhodko, *Phys. Lett. A*, **366**, 422 (2007);
V. M. Lashkin, *Phys. Rev. A*, **77**, 025602 (2008);
V. M. Lashkin, *Phys. Rev. A*, **78**, 033603 (2008).
32. X. Liu, L. J. Qian, F. W. Wise, *Phys. Rev. Lett.*, **82**, 4631 (1999).

33. D. Mihalache *et al.*, Phys. Rev. E, **70**, 055603 (2004).
34. D. Mihalache *et al.*, Phys. Rev. Lett., **95**, 023902 (2005).
35. D. Mihalache *et al.*, Phys. Rev. A, **72**, 021601 (2005).
36. D. Mihalache *et al.*, Phys. Rev. E, **74**, 047601 (2006).
37. H. Leblond, B. A. Malomed, D. Mihalache, Phys. Rev. E, **76**, 026604 (2007).
38. N. Akhmediev, A. Ankiewicz (Eds.), *Dissipative Solitons: From Optics to Biology and Medicine*, Lect. Notes Phys. **751**, Springer, Berlin, 2008;
N. Akhmediev, A. Ankiewicz (Eds.), *Dissipative Solitons*, Lect. Notes Phys. **661**, Springer, Berlin, 2005.
39. I. S. Aranson, L. Kramer, Rev. Mod. Phys., **74**, 99 (2002);
P. Mandel, M. Tlidi, J. Opt. B: Quantum Semiclass. Opt., **6**, R60 (2004);
B. A. Malomed, in *Encyclopedia of Nonlinear Science*, p. 157, A. Scott (Ed.), Routledge, New York, 2005.
40. L.-C. Crasovan, B. A. Malomed, D. Mihalache, Phys. Rev. E, **63**, 016605 (2001);
L.-C. Crasovan, B. A. Malomed, D. Mihalache, Phys. Lett. A, **289**, 59 (2001).
41. D. Mihalache *et al.*, Phys. Rev. Lett., **97**, 073904 (2006).
42. D. Mihalache, D. Mazilu, F. Lederer, H. Leblond, B. A. Malomed, Phys. Rev. A, **75**, 033811 (2007);
D. Mihalache *et al.*, Phys. Rev. A, **76**, 045803 (2007).
43. P. Grelu, J. M. Soto-Crespo, N. Akhmediev, Opt. Express, **13**, 9352 (2005);
J. M. Soto-Crespo, N. Akhmediev, P. Grelu, Phys. Rev. E, **74**, 046612 (2006).
44. V. Skarka, N. B. Aleksić, Phys. Rev. Lett., **96**, 013903 (2006).
45. D. Mihalache, Cent. Eur. J. Phys., **6**, 582 (2008);
D. Mihalache, D. Mazilu, Rom. Rep. Phys., **60**, 749 (2008).
46. J. M. Soto-Crespo, P. Grelu, N. Akhmediev, Opt. Express, **14**, 4013 (2006);
N. Akhmediev, J. M. Soto-Crespo, P. Grelu, Chaos, **17**, 037112 (2007).
47. D. Mihalache, D. Mazilu, F. Lederer, H. Leblond, B. A. Malomed, Phys. Rev. A, **77**, 033817 (2008); Phys. Rev. E, **78**, 056601 (2008).
48. W. J. Tomlinson, Opt. Lett., **5**, 323 (1980);
V. M. Agranovich, V. S. Babichenko, V. Y. Chernyak, JETP Lett., **32**, 512 (1980).
49. V. K. Fedyanin, D. Mihalache, Z. Phys. B, **47**, 167 (1982);
D. Mihalache, R. G. Nazmitdinov, V. K. Fedyanin, Physica Scripta, **29**, 269 (1984);
D. Mihalache, D. Mazilu, H. Totia, Physica Scripta, **30**, 335 (1984).
50. U. Langbein, F. Lederer, H.-E. Ponath, Opt. Commun., **46**, 167 (1983).
51. G. I. Stegeman, C. T. Seaton, J. Chilwell, S. D. Smith, Appl. Phys. Lett., **44**, 830 (1984).
52. N. N. Akhmediev, V. I. Korneyev, Y. V. Kuzmenko, Zh. Eksp. Teor. Fiz., **88**, 107 (1985) [Sov. Phys. JETP, **61**, 62 (1985)].
53. F. Lederer, D. Mihalache, Solid State Commun., **59**, 151 (1986);
D. Mihalache, D. Mazilu, F. Lederer, Opt. Commun., **59**, 391 (1986);
D. Mihalache *et al.*, Opt. Lett., **12**, 187 (1987).
54. D. Mihalache, M. Bertolotti, C. Sibilio, Prog. Opt., **27**, 229 (1989).
55. A. D. Boardman, P. Egan, F. Lederer, U. Langbein, D. Mihalache, "Third-order nonlinear electromagnetic TE and TM guided waves," in: *Nonlinear Surface Electromagnetic Phenomena*, H.-E. Ponath, and G. I. Stegeman eds., Elsevier Science Publishers B.V., Amsterdam, 1991, pp. 73–287.
56. F. Lederer, L. Leine, R. Muschall, T. Peschel, C. Schmidt-Hattenberger, U. Trutschel, A. D. Boardman, C. Wächter, Opt. Commun., **99**, 95 (1993).
57. K. G. Makris, S. Suntsov, D. N. Christodoulides, G. I. Stegeman, A. Haché, Opt. Lett., **30**, 2466 (2005).

58. Ya. V. Kartashov, V. V. Vysloukh, L. Torner, *Phys. Rev. Lett.*, **96**, 073901 (2006).
59. S. Suntsov, K. G. Makris, D. N. Christodoulides, G. I. Stegeman, A. Haché, R. Morandotti, H. Yang, G. Salamo, M. Sorel, *Phys. Rev. Lett.*, **96**, 063901 (2006).
60. C. R. Rosberg, D. N. Neshev, W. Krolikowski, A. Mitchell, R. A. Vicencio, M. I. Molina, Yu. S. Kivshar, *Phys. Rev. Lett.*, **97**, 083901 (2006).
61. M. I. Molina, R. A. Vicencio, Yu. S. Kivshar, *Opt. Lett.*, **31**, 1693 (2006).
62. Y. V. Kartashov, L. Torner, and V. A. Vysloukh, *Opt. Lett.* **31**, 2595 (2006);
Y. V. Kartashov, F. Ye, V. A. Vysloukh, L. Torner, *Opt. Lett.*, **32**, 2260 (2007).
63. Y. Kominis, A. Papadopoulos, K. Hizanidis, *Opt. Express*, **15**, 10041 (2007).
64. M. I. Molina, Y. V. Kartashov, L. Torner, Yu. S. Kivshar, *Opt. Lett.*, **32**, 2668 (2007).
65. Z. Xu, Yu. S. Kivshar, *Opt. Lett.*, **33**, 2551 (2008).
66. E. Smirnov, M. Stepić, C. E. Rütter, D. Kip, V. Shandarov, *Opt. Lett.*, **31**, 2338 (2006).
67. B. Alfassi, C. Rotschild, O. Manela, M. Segev, D. N. Christodoulides, *Phys. Rev. Lett.*, **98**, 213901 (2007).
68. A. Szameit, Y. V. Kartashov, F. Dreisow, M. Heinrich, T. Pertsch, S. Nolte, A. Tünnermann, V. A. Vysloukh, L. Torner, *Opt. Lett.*, **33**, 1132 (2008).
69. X. Wang, A. Samodurov, Z. Chen, *Opt. Lett.*, **33**, 1240 (2008).
70. S. Suntsov *et al.*, *J. Nonl. Opt. Phys. & Mat.*, **16**, 401 (2007);
F. Lederer, G. I. Stegeman, D. N. Christodoulides, G. Assanto, M. Segev, Y. Silberberg, *Phys. Rep.*, **463**, 1 (2008);
Yu. S. Kivshar, *Laser Phys. Lett.*, **5**, 703 (2008).
71. D. Mihalache, D. Mazilu, F. Lederer, Yu. S. Kivshar, *Opt. Express*, **15**, 589 (2007).
72. D. Mihalache, D. Mazilu, F. Lederer, Yu. S. Kivshar, *Opt. Lett.*, **32**, 2091 (2007).
73. D. Mihalache, D. Mazilu, Yu. S. Kivshar, F. Lederer, *Opt. Express*, **15**, 10718 (2007).
74. D. Mihalache, D. Mazilu, F. Lederer, Yu. S. Kivshar, *Opt. Lett.*, **32**, 3173 (2007).
75. A. B. Aceves, C. De Angelis, A. M. Rubenchik, S. K. Turitsyn, *Opt. Lett.*, **19**, 329 (1994);
E. W. Laedke, K.H. Spatschek, S. K. Turitsyn, *Phys. Rev. Lett.*, **73**, 1055 (1994);
A. B. Aceves, G. G. Luther, C. De Angelis, A. M. Rubenchik, S. K. Turitsyn, *Phys. Rev. Lett.*, **75**, 73 (1995);
A. V. Buryak, N. N. Akhmediev, *IEEE J. Quantum Electron.*, **31**, 682 (1995).
76. Z. Xu, Y. V. Kartashov, L. C. Crasovan, D. Mihalache, L. Torner, *Phys. Rev. E*, **70**, 066618 (2004).
77. D. Mihalache, D. Mazilu, F. Lederer, Yu. S. Kivshar, *Phys. Rev. A*, **77**, 043828 (2008).
78. D. Mihalache, D. Mazilu, F. Lederer, Yu. S. Kivshar, *Phys. Rev. E*, **78**, 056602 (2008).
79. N. K. Efremidis, D. N. Christodoulides, *Phys. Rev. E*, **67**, 026606 (2003).
80. E. A. Ultanir, G. I. Stegeman, D. Michaelis, C. H. Lange, F. Lederer, *Phys. Rev. Lett.*, **90**, 253903 (2003).
81. U. Peschel, O. Egorov, F. Lederer, *Opt. Lett.*, **29**, 1909 (2004).
82. N. K. Efremidis, D. N. Christodoulides, K. Hizanidis, *Phys. Rev. A*, **76**, 043839 (2007).
83. Yu. V. Bludov, V. V. Konotop, *Phys. Rev. E*, **76**, 046604 (2007).
84. Q. E. Hoq, R. Carretero-Gonzalez, P. G. Kevrekidis, B. A. Malomed, D. J. Frantzeskakis, Yu. V. Bludov, V. V. Konotop, *Phys. Rev. E*, **78**, 036605 (2008).
85. C. J. Benton, A. V. Gorbach, D. V. Skryabin, *Phys. Rev. A*, **78**, 033818 (2008).
86. H. Leblond, B. A. Malomed, D. Mihalache, *Phys. Rev. A*, **77**, 063804 (2008).
87. N. C. Panoiu, R. M. Osgood, B. A. Malomed, *Opt. Lett.*, **31**, 1097 (2006);
N. C. Panoiu, B. A. Malomed, R. M. Osgood, *Phys. Rev. A*, **78**, 013801 (2008).
88. F. Kh. Abdullaev, Yu. V. Bludov, S. V. Dmitriev, P. G. Kevrekidis, V. V. Konotop, *Phys. Rev. E*, **77**, 016604 (2008).

89. K. G. Makris, J. Hudock, D. N. Christodoulides, G. I. Stegeman, O. Manela, M. Segev, *Opt. Lett.*, **31**, 2774 (2006).
90. M. I. Molina, Yu. S. Kivshar, *Phys. Lett. A*, **362**, 280 (2007).
91. A. A. Sukhorukov, Yu. S. Kivshar, *Opt. Lett.* **27**, 2112 (2002); A. A. Sukhorukov, Yu. S. Kivshar, *Opt. Lett.* **28**, 2345 (2003).
92. R. Morandotti, D. Mandelik, Y. Silberberg, J. S. Aitchison, M. Sorel, D. N. Christodoulides, A. A. Sukhorukov, Yu. S. Kivshar, *Opt. Lett.* **29**, 2890 (2004).
93. K. G. Makris, J. Hudock, D. N. Christodoulides, G. Stegeman, O. Manela, M. Segev, *Opt. Lett.*, **31**, 2774 (2006).
94. R. A. Vicencio, S. Flach, M. I. Molina, Yu. S. Kivshar, *Phys. Lett. A*, **364**, 274 (2007).
95. H. Susanto, P. G. Kevrekidis, B. A. Malomed, R. Carretero-González, D. J. Franzesckakis, *Phys. Rev. E*, **75**, 056605 (2007).
96. X. Wang, A. Bezryadina, Z. Chen, K. G. Makris, D. N. Christodoulides, G. I. Stegeman, *Phys. Rev. Lett.*, **98**, 123903 (2007).
97. A. Szameit, Y. V. Kartashov, F. Dreisow, T. Pertsch, S. Nolte, A. Tünnermann, L. Torner, *Phys. Rev. Lett.*, **98**, 173903 (2007).
98. D. Mihalache, D. Mazilu, F. Lederer, Y. S. Kivshar, *Phys. Rev. A*, **79**, 013811 (2009).